Resolving the Rise and Fall of Star Formation in Galaxies
Proceedings IAU Symposium No. 373, 2023
T. Wong & W.-T. Kim, eds.
doi:10.1017/S1743921322003787

High [OIII] luminosities from star formation and shocks in z∼6 quasars

Bomee Lee[1] **and Ranga-Ram Chary**[2]

[1]Korea Astronomy and Space Science Institute, Daedeokdae-ro 776, Yuseong-gu, Daejeon 34055, Republic of Korea; email: bomee@kasi.re.kr

[2]MS314-6, Infrared Processing and Analysis Center, California Institute of Technology, Pasadena, CA 91125, USA

Abstract. We use archival WISE and Spitzer photometry to derive optical emission line fluxes for a sample of distant quasars at z∼6. We find evidence for exceptionally high equivalent width [OIII] emission (rest-frame EW∼400Å) similar to that inferred for star-forming galaxies at similar redshifts. The median Hα and Hβ equivalent widths are derived to be ∼400Å and ∼100Å respectively, and are consistent with values seen among quasars in the local Universe, and at $z \sim 2$. After accounting for the contribution of photoionization in the broad line regions of quasars, we suggest that the narrow [OIII] emission likely arises from feedback due to massive star-formation in the quasar host. Forthcoming mid-infrared spectroscopy with the James Webb Space Telescope will help constrain the physical conditions in quasar hosts further.

Keywords. high redshifts, quasars, emission lines, galaxy formation/evolution

1. Introduction

Emission lines from ionized gas, particularly Hα, Hβ and [OIII] are a tracer of ISM conditions, particularly the magnetic field strength, the shock velocity, gas density and metallicity (Allen et al. 2008). At high redshifts, these diagnostic lines are redshifted to mid-infrared wavelengths. Although this will be remedied imminently through spectroscopic observations with the *James Webb Space Telescope*, it has not been possible thus far, to place constraints on the line strengths. In the case of star-forming, emission-line galaxies at high redshift, a pioneering approach which utilized the excess emission in broad, mid-infrared bandpasses yielded strong evidence for high equivalent width (EW) nebular emission but these studies were limited by signal to noise ratio (SNR; e.g. Chary et al. 2005; Faisst et al. 2016).

In comparison, quasars, by being the most luminous sources in the distant Universe, have multi-wavelength photometry that has much higher SNR than for most star-forming galaxies. In this study, we leverage this high quality photometry to derive rest-frame optical emission-line properties of a sample of $z \sim 6$ quasars.

2. Estimates of the rest-frame optical emission line strengths

Our initial sample consists of a list of 520 quasars at $z > 5$ that have been spectroscopically confirmed (Ross & Cross 2020). We collect multi-wavelength photometric data between the optical $y-$band ($\sim 0.9\,\mu$m) and 8 μm from archival imaging data on those $z > 5$ quasars including UKIRT/WFCAM and VISTA/VIRCAM, Pan-STARRS1 DR2, *Spitzer*/IRAC, and WISE. We select 53 quasars at $5.03 < z < 6.3$ having SNR> 5 in both IRAC 1 (3.6 μm) and 2 (4.5 μm) channels (see Lee & Chary (2022) for more details).

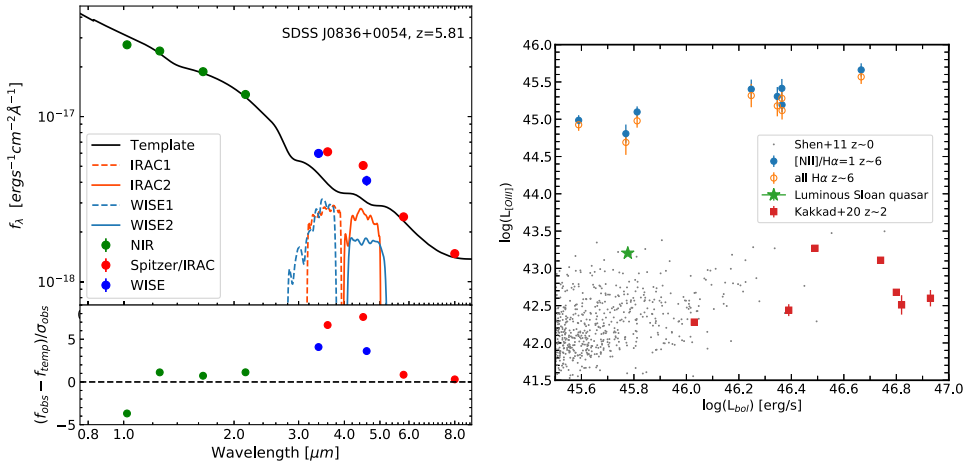

Figure 1. Left: An example fit of SDSS J0836+0054, a quasar at z = 5.81 with its observed photometry. Black line represents the continuum template best-fitted to near-IR bands and IRAC 5.8 and 8μm bands. The transmission curves of IRAC 3.6 and 4.5μm (orange) and WISE 3.3 and 4.6μm bands (light blue) are overplotted. Bottom panel: The difference between observed flux (f_{obs}) and continuum flux (f_{temp}) as a function of wavelength. One can clearly see the bumps between 3 and 5 μm due to [OIII] and Hβ in the $\sim$3.5μm bandpasses and Hα+[NII] in the $\sim$4.5μm bandpasses. **Right**: Bolometric Luminosity vs our derived [OIII] luminosity of 8 quasars at z$\sim$6 (blue and orange), AGNs from SDSS DR7 (grey), and z$\sim$2 quasars from VLT/SINFONI (red). Empty orange and filled blue circles represent the range in [OIII] luminosities for the two broad-line region scenarios discussed in the text. A local AGN having similar [OIII]/Hβ ratio as $z \sim 6$ quasars is the green star.

The entrance of redshifted emission lines, such as Hα, [NII], Hβ, and [OIII], in $z > 5$ galaxies, can introduce a photometric excess in certain bands. These lines introduce a significant difference between the observed photometry and the underlying continuum flux density, if the EW of the lines is high. Thus, if we can fit for the underlying continuum flux density using templates, we can obtain an estimate of the emission line fluxes using the excess emission in the different bands. As an example, for the z = 5.81 quasar shown in the left of Figure 1, the Hα line flux can be estimated from the photometry in the IRAC 2 and WISE 2 bands, while Hβ+[OIII] can be estimated with IRAC 1 and WISE 1 bands. For typical quasars, the Hydrogen Balmer lines arise from photoionization in the broad line region (BLR). As a result it is difficult to separate the [NII] and [OIII] narrow-line emission from the broad Hydrogen lines. In order to assess if there is a component of narrow-line emission in the photometry, we adopt two scenarios: 1) where the BLR Hα emission accounts for half the IRAC2 and WISE2 photometric excess (with the NLR accounting for the rest), and 2) where the BLR accounts for all the excess. Since we cannot fit spectra to measure line widths, we fix FWHM = 3400km/s for all lines. FWHM = $3400 km/s$ is chosen as a median FWHM of the MgII line in 82 quasars at $4.5 < z < 6.4$ (see Lee & Chary (2022) for references) and assumes a correlation of FWHM between $MgII$ and Hα lines (Jun et al. 2015).

With these assumptions and a Gaussian profile for the line, we derive the $H\alpha$ line fluxes using the excess emission at IRAC2 and/or WISE 2. Hβ is derived by assuming an Hα/Hβ= 2.86 (i.e. no dust). We derive [OIII] after subtracting the Hβ contribution from the excess emission in IRAC 1 and/or WISE 1. Depending on the redshift, the final line flux is the SNR-weighted line flux from both the IRAC 1 (IRAC2) and WISE 1 (WISE2) excess, when available. We use a Monte Carlo simulation to produce robust

https://doi.org/10.1017/S1743921322003787 Published online by Cambridge University Press

uncertainty estimates on the fitted emission lines. As a result, we are able to constrain Hβ and [OIII] line fluxes for only a subset of 33 quasars at $5.03 < z < 6.3$ due to large photometric uncertainties in most of cases, and inadequacy of the templates in a small subset of cases.

3. Optical emission line constraints at z $\sim$ 6

To investigate the physical characteristics of z > 5 quasars, we further restrict our sample to those which have $SNR > 3$ in $H\alpha$ and [OIII]. We have a final sample of 8 quasars at $5.03 < z < 6.23$ with a median redshift of $z = 5.94$ and compute the [OIII] luminosity of them (Figure 1 right panel). The median bolometric luminosity of this sample of quasars is 2×10^{46} erg/s with a range of $3.9 \times 10^{45} < L_{AGN}\ [erg/s] < 4.6 \times 10^{46}$. The derived median rest-frame EWs of Hα, Hβ and [OIII] are 400Å, 100Å and 440Å respectively. The median derived [OIII] luminosity is 2×10^{45} erg/s. [OIII] luminosities of $z \sim 6$ quasars are about two orders of magnitude higher than luminous local quasars (Shen et al. 2011) or z$\sim$ 2 quasars studied with VLT/SINFONI (Vietri et al. 2020) (Figure 1). Moreover, we find rest-frame Hα EWs of $\sim$300-800Å at luminosities of $\sim 10^{46}$ erg s^{-1}. This is in good agreement with the values derived for $z > 5$ quasars, using a similar methodology by Leipski et al. (2014), and similar to the Hα EWs of Sloan quasars (Shen et al. 2011). The median Hβ rest-frame EW of the local SDSS quasars is 100Å (Shen et al. 2011), similar to our sample, implying that much of the excess in the bluer bandpass is indeed because of the [OIII] doublet.

4. Physical Implication for $z \sim 6$ Quasars

The photometric excess that we are measuring is the sum of emission from the narrow-line region (NLR), the broad-line region (BLR) and from stellar/ISM emission. Given the luminosity of the sample, the BLR is likely dominating the Hydrogen Balmer emission-line luminosities. For instance, in Shen et al. (2011), the local quasars show broad-line luminosities that are $\sim$20 times the narrow-line luminosities for Hα and Hβ. Much of the broad line emission is powered by photoionization by the central source. However, local quasar hosts are relatively quiescent with low-levels of ambient star-formation compared to our high-z galaxy sample (Zakamska et al. 2016). Our measurement of the enhanced [OIII] emission is surprising, implying a significant component arising from the NLR and from star-formation (Vietri et al. 2020). In $z \sim 2$ quasars of comparable bolometric luminosities as the sources studied here, the NLR [OIII] line luminosities are $\sim 10^{43}$ erg s^{-1} (Kakkad et al. 2020). The narrow component of [OIII] in those systems account for about 35% of the total [OIII] emission. In contrast, the median [OIII] luminosity of our sample is $10^{45.3}$ erg s^{-1}. Since the EWs of the Balmer lines are consistent between low- and high-z quasars, the implication is that the high [OIII] luminosity of our sample arises from an additional component, likely star-formation, rather that the quasar-powered ionized outflows noted by Kakkad et al. (2020). Spatially resolved measurements of the kinematics of [OIII] emission are required to confirm this explanation although the compactness of the stellar population at high-z (<1 kpc) will make it challenging to resolve stellar emission against the brightness of the quasar.

The large [OIII] EW and luminosity of $z \sim 6$ quasar hosts compared to $z \sim 2$, is similar to what has been inferred for star-forming galaxies (Endsley et al. 2021) who present evidence that at redshifts ~ 7, 50% of star-forming galaxies have rest-frame [OIII] EWs greater than 500Å. Since it is challenging to obtain such high [OIII]/Hβ ratios purely from photoionization models (Baskin & Laor 2005), strong star-formation-driven outflows powering radiative shocks are required to explain the emission. Future, mid-infrared spectroscopy with JWST, will be crucial to measure the kinematics of these lines to distinguish

https://doi.org/10.1017/S1743921322003787 Published online by Cambridge University Press

the contribution of the BLR, and NLR and to accurately constrain the metallicity, and magnetic field strength.

References

Allen, M. G., Groves, B. A., Dopita, M. A., Sutherland, R. S., Kewley, L. J. 2008, ApJs, 178, 20

Baskin, A. and Laor, A. 2005, MNRAS, 358, 1043

Chary, R.-R., Stern, D., & Eisenhardt, P. 2005, ApJL, 635, L5. doi:10.1086/499205

Endsley, R., Stark, D. P., Chevallard, J., et al. 2021, MNRAS, 500, 5229. doi:10.1093/mnras/staa3370

Faisst, A. L., Capak, P., Hsieh, B. C., et al. 2016, ApJ, 821, 122. doi:10.3847/0004-637X/821/2/122

Jun, H. D., Im, M., Lee, H. M., Ohyama, Y. et al, 2015, ApJ, 806, 109

Kakkad, D., Mainieri, V., Vietri, G., et al. 2020, *A&A*, 642, A147. doi:10.1051/0004-6361/202038551

Lee, B., & Chary, R., 2022, arXiv:2207.07290

Leipski, C., Meisenheimer, K., Walter, F., et al. 2014, ApJ, 785, 154. doi:10.1088/0004-637X/785/2/154

Ross, N. P., Cross, N. J. G. 2020, MNRAS, 494, 789

Shen, Y., Richards, G. T., Strauss, M. A., et al. 2011, ApJs 194, 45. doi:10.1088/0067-0049/194/2/45

Vietri, G., Mainieri, V., Kakkad, D., et al. 2020, *A&A*, 644, A175. doi:10.1051/0004-6361/202039136

Zakamska, N. L., Lampayan, K., Petric, A., et al. 2016, MNRAS, 455, 4191. doi:10.1093/mnras/stv2571